Prediction of the ossification process in fracture healing employing ultrasound stimulation

Maria G. Vavva, Konstantinos N. Grivas, Aurélie Carlier, Demosthenes Polyzos, Liesbet Geris, Hans Van Oosterwyck, Dimitrios I. Fotiadis, *Senior Member, IEEE*

Abstract— **The bone healing process involves a sequence of cellular actions and interactions, regulated by biochemical and mechanical signals. Experimental studies have shown that ultrasound accelerates bone ossification and has a multiple influence on angiogenesis and bone healing underlying mechanisms. In this study we present a mathematical model for deriving predictions of bone healing under the presence of ultrasound. The primary objective is to account for the ultrasound effect on angiogenesis and more specifically on the transport of the Vascular Endothelial Growth Factor (VEGF). The model consists of i) partial differential equations which describe the spatiotemporal evolution cells, growth factors, tissues and ultrasound acoustic pressure and ii) velocity equations of endothelial tip cells which determine the development of the blood vessel network. The results demonstrated that ultrasound accelerates bone healing. In addition the evolution of the average osteoblast, vascular and bone matrix densities were also enhanced. The proposed model could be regarded as a step towards the ultrasonic evaluation of bone since it can provide quantitative criteria for the monitoring of bone healing and angiogenesis.**

I. Introduction

FRACTURE healing is a complicated process that includes a multiple cellular mechanisms and stages. The process begins with an inflammatory stage, which leads to the creation of the callus and the differentiation of tissues within the callus and is completed with the callus resorption and bone remodeling.

More specifically in the secondary type of bone healing the inflammatory stage starts when a fracture occurs and includes the formation of a hematoma and cell death caused by the disruption of the local blood supply. This is followed by an aseptic inflammatory response which leads to the absorption of the necrotic tissue, revascularization of the region as well as cell proliferation and differentiation. Angiogenesis is then initiated from the release of the inflammatory cytokines triggering the activities of osteoclasts and macrophages [1, 2, 3]. In the second stage, progenitor cells produce new cells which deliver fibroblasts and intercellular constituents for the development of the soft granulation tissue [4]. In the third stage i.e., the bone callus formation, new chondrocytes and osteoblasts are created within the granulation tissue [5, 6].

The fracture callus tissue is then created which is divided in the hard callus, where intramembranous ossification occurs and the soft callus, where endochondral ossification takes place [7]. Inside the initial callus and close to the fracture site, osteochondral cells differentiate into chondrocytes. Thereafter After one or two weeks, chondrocytes divide and synthesize cartilage [8] and the callus mostly contains hypertrophic chondrocytes. New blood vessels are developed in the calcified cartilage which is then replaced with ossified tissue and woven bone through endochondral ossification. In the final stage bone remodeling occurs during which the external callus is remodeled into cortical bone [8]. After completion of this stage the bone gains its original size, shape and strength.

Angiogenesis is a vital part of bone healing, since it re-establishes blood flow at the fracture site, preventing thus ischaemic necrosis and allowing repair. Many growth factors, including fibroblast growth factor (FGF), bone morphogenetic protein (BMP), transforming growth factor (TGF), and vascular endothelial growth factor (VEGF) families play a key angiogenic and osteogenic role during fracture healing [9, 10]. These factors are produced by and responded to by various cell types existing at the fracture site [9].

Although the exact mechanisms behind angiogenesis are not yet fully understood VEGF is known to play a key role [11]. VEGF is produced by cells in hypoxia and diffuses towards existing blood vessels as well as by hypertrophic chondrocytes triggering the endochondral ossification pathway. When VEGF reaches nearby blood vessels it will activate endothelial cells to express "tip cell" phenotype or become "stalk cells". A tip cell

M.G. Vavva, K. N. Grivas and D. Polyzos are with the the Department of Mechanical Engineering and Aeronautics, University of Patras, GR 26 500 Patras, Greece, (correspondence e-mail: grivas@mech.upatras.gr, mvavva@gmail.com).

D.I. Fotiadis is with the Unit of Medical Technology and Intelligent Information Systems, University of Ioannina, GR 45110, Ioannina, Greece and the Biomedical Research Institute – FORTH, Ioannina, Greece (phone: 0030-2651008803;fax:00302651008889;correspondence e-mail:fotiadis@cc.uoi.gr).

A. Carlier, L. Geris and H.Van Oosterwyck are with the Department of Mechanical Engineering, KU Leuven, Leuven, Belgium and the Biomechanics Research Unit, University of Liège, Liège, Belgium (correspondence e-mail: Aurelie.carlier@mech.kuleuven.be, Liesbet.geris@ulg.ac.be, hans.vanoosterwyck@mech.kuleuven.be)

senses microenvironmental stimuli by using filopodia and moves away from its mother vessel giving lead to a new blood vessel branch. The newly developing branches are lengthened through chemotaxis i.e., the movement of the tip cell towards the source of VEGF. As the cell attaches and moves along fibers in the extracellular matrix, there is also a haptotactic component of tip cell motion [12, 13].

A. Computational Models of Bone Healing including Angiogenesis

Several computational studies have been performed to simulate bone healing in order to elucidate the underlying mechanisms of cell activities and angiogenesis [14, 15]. In 2005 a fuzzy logic model was proposed to model fracture healing [16] and the fracture vascularity. This study was based on the study of [17]. Angiogenesis process was modelled via a single variable s different basic mechanoregulatory rules. The fuzzy logic rules of this study were later adapted by Chen et al. [18] in order to model nutrition supply in the fracture site instead of vascularity. A continuous mathematical model of bone regeneration describing healing has been also presented by Geris et al. [19] using a system of partial differential equations in which the unknown variables were the densities of cell types, growth factors and tissues. The spatiotemporal development of endothelial cell concentration and vascular density was used to model the angiogenesis process. The predicted healing process was in accordance with experimental observations. However, the authors pointed out that the discrete nature of vasculature cannot be fully described by continuous variables. To this end the same group further extended their work by adapting the system of PDEs so as to describe vascularization with a discrete variable [12]. The proposed angiogenesis model was based on a previous deterministic hybrid model [13], in which a set of PDEs describes the velocity of each tip cell, and also simulated sprout dynamics i.e., blood vessel growth and branching.

A lattice-based model has been also presented to describe tissue differentiation and angiogenesis in a bone/implant fracture under shear loading [20]. This study was based in the work of Anderson and Chaplain [21] in which the tip cell motion was simulated as a probabilistic biased random walk. An additional tissue differentiation stimulus i.e., the oxygen concentration level, was inserted in the mechanoregulatory algorithm in order to account for angiogenesis. More specifically oxygen diffusion is limited to a few hundred micrometers from capillaries. Higher loads were found to lead to lower vascularization rates and thus delayed bone formation. The results were in accordance with experimental findings. This model was also used for the evaluation of the effect of cell seeding and mechanical loading on scaffolds [22] and the investigation of the differences in bone repair between small and large animals [20].

A similar method was also used in [23] for the determination of the acceleration of the tip cells. A rule-based model of sprouting angiogenesis has been also reported in [24] where the elongation and proliferation of stalk cells as well as the effect of Notch factor production are explicitly simulated.

B. Effects of Ultrasound on Bone Healing Mechanisms

Quantitative ultrasound has been widely used for the investigation of the underlying mechanisms of the ultrasound effect and the assessment of bone healing process. Physically ultrasound induces mechanical forces at the cellular level which have been shown to regulate bone formation [1, 25]. In an experimental study [26] the authors by applying (Low Intensity Pulsed Ultrasound) LIPUS on osteoporotic fracture rat models found an earlier bridging of the fracture gap and increased amount of callus formation as compared with the control group. In addition they also found higher amounts of cartilage at weeks 2-4 post-fracture in the LIPUS group suggesting that the earlier callus formation may be attributed to enhanced endochondral ossification. In a later work [27] aiming at the investigation of the effect of different LIPUS intensities on fracture healing it was found that low-density bone volume fraction was significantly higher in the group treated with LIPUS at $I_{SATA} = 30mW/cm^2$ than in the control group. LIPUS at higher intensity was found not to further accelerate bone healing. US has been also found to accelerate primary callus formation in femur and fibular osteotomies in rabbits [28]. More specifically it was observed that for the first 10–12 days post-fracture, US caused a rapid increase in callus formation which was then stabilized. On the other hand, this rapid increase in callus formation in control osteotomies occurred at approximately 2 weeks after fracture. In another study [29] by applying US on rat femoral fractures it was found that chondrocytes exhibit a significant increase in aggrecan gene expression after exposure to US which is correlated with chondrogenesis [30]. Furthermore, US was also found to cause earlier falls in the expression of the same genes [29], which has been found to be correlated with cartilage hypertrophy and endochondral ossification [40]. The authors stated that one possible mechanism is the direct US stimulation of the chondrocytes [31, 32, 33] or the fact that US leads to an enhanced calcium uptake as shown in [31]. Zhang et al., [34] by applying Pulsed Low Intensity Ultrasound (PLIUS) separately to cultured proximal and distal parts of chick sternum found that ultrasound increases the expression of type X collagen from hypertrophic chondrocytes that are at the terminal stage of differentiation.

As regards angiogenesis ultrasound has been shown to significantly enhance blood vessel formation due to an increase of the levels of cytokines', fibroblast growth factor, and vascular endothelial growth factor (VEGF), which are related to angiogenesis. In two experimental studies of ultrasound application on human osteoblasts, gingival fibroblasts and blood mononuclear cells [35, 36] cytokines that are related with angiogenesis were found significantly stimulated in osteoblasts, and VEGF levels were found increased. Increased VGEF expression at week 4 to 8 post-fracture indicating increased amounts of new blood vessel formation is also reported in [26]. The authors suggested that angiogenesis is enhanced by LIPUS during the remodeling phase of healing in osteoporotic fractures. In another study [37] it was found that low-intensity power Doppler ultrasound application on ulnar osteotomies in dogs caused increased vascularity in the fracture site which enhances the delivery of growth factors and cytokines

necessary for the healing process.

Furthermore it has been also shown that the US frequency plays vital role in angiogenesis and that during the inflammatory stage the main US receptors in the granulation tissue are the macrophage [38-39]. In two other studies [40-41] macrophages have been shown to induce angiogenesis in vivo by producing angiogenic factors, and to increase the levels of endothelial cell proliferation in vitro. In another study of US application on chick chorioallantoic membrane [42] it was also showed that ultrasound can induce angiogenesis in vivo. The study also showed that effect is more pronounced for specific US intensities and frequencies.

C. Computational Studies of Ultrasonic Assessment of Intact and Healing Bones

A large number of animal and clinical studies have also investigated the ability of quantitative ultrasound to monitor the healing process [43]. These studies have demonstrated that the propagation velocity across fractured bones can be used as an indicator of healing [43]. Furthermore the technique of ultrasound axial transmission, has been proven effective in providing ultrasonic parameters that are related to long bone's mechanical and geometrical properties.

Researchers have also recently developed computational models of ultrasound wave propagation in bones aiming to further enhance the monitoring capabilities of ultrasound. Nevertheless these models are currently focused on describing realistic bone geometries and their mechanical properties at a meso- and macro-level [1-3]. Furthermore they primarily aim at investigating the possibility of employing novel means of evaluating the mechanical properties of bone and monitoring the healing course without making any attempt to describe the underlying physiological healing phenomena. On the other hand mechanobiological and mathematical models have been extensively used to 1) describe the mechanisms by which mechanical loads regulate biological processes through signals to cells and 2) simulate the complex biological processes, such as bone repair which are difficult to be experimentally and clinically studied. Therefore such models can aid in providing novel insights and fundamental understanding of the influence of US on bone healing.

In this work we present a deterministic hybrid model for bone healing and angiogenesis predictions under the effect of ultrasound. The model is based on the work of [12] consisting of partial differential equations which describe the spatiotemporal evolution of soft tissues, bone and the development of blood vessel network. We assume that ultrasound primarily affects the transport of VEGF. An extensive sensitivity analysis for the newly introduced parameters is evaluated. The results are corroborated by comparisons with previous studies in order to elucidate the exact cellular mechanisms that lead to acceleration of bone healing due to ultrasound.

II. MATERIALS AND METHODS

A. Model overview

The proposed model of healing includes 12 differential equations as presented in [12] describing the spatiotemporal variation of mesenchymal stem cells (c_m), fibroblasts (c_f), chondrocytes (c_c), osteoblasts (c_b), fibrous extracellular matrix (m_f), cartilaginous extracellular matrix (m_c), bone extracellular matrix (m_b), generic osteogenic (g_b), chondrogenic (g_c) and vascular growth factors (g_v) as well as the concentration of oxygen and nutrients (n). To represent the sprout dynamics the discrete variable c_v is used. The partial differential equations (PDE) are of taxis-diffusion-reaction type:

$$\frac{\partial c_m}{\partial t} = \nabla \cdot \left(D_m \nabla c_m - C_{mCT} c_m \nabla \left(g_b + g_v \right) - C_{mHT} c_m \nabla m \right), \\ + A_m c_m (1 - \alpha_m c_m) - \mathrm{F}_1 c_m - \mathrm{F}_2 c_m - \mathrm{F}_4 c_m \tag{1}$$

$$\frac{\partial c_f}{\partial t} = \nabla \cdot \left(D_f \nabla c_f - C_f c_f \nabla g_b \right) + A_f c_f (1 - \alpha_f \, c_f) \\ + \mathrm{F}_4 \, c_m - \mathrm{F}_3 \, d_f c_f, \tag{2}$$

$$\frac{\partial c_c}{\partial t} = A_c c_c (1 - \alpha_c \, c_c) + \mathrm{F}_2 \, c_m - \mathrm{F}_3 \, c_m, \tag{3}$$

$$\frac{\partial c_b}{\partial t} = A_b c_b (1 - \alpha_b \, c_b) + \mathrm{F}_1 \, c_m + \mathrm{F}_3 \, c_c - d_b \, c_b, \tag{4}$$

$$\frac{\partial m_f}{\partial t} = P_{fs} (1 - \kappa_f m_f) \mathrm{c}_f - Q_f m_f m_c \, \mathrm{c}_b, \tag{5}$$

$$\frac{\partial m_c}{\partial t} = P_{cs} (1 - \kappa_c m_c) \mathrm{c}_c - Q_c m_c c_b, \tag{6}$$

$$\frac{\partial m_b}{\partial t} = P_{bs} (1 - \kappa_b m_b) \mathrm{c}_b, \tag{7}$$

$$\frac{\partial g_c}{\partial t} = \nabla \cdot \left(D_{gc} \nabla g_c \right) + E_{gc} c_c - d_{gc} g_c, \tag{8}$$

$$\frac{\partial g_b}{\partial t} = \nabla \cdot \left(D_{gb} \nabla g_b \right) + E_{gb} c_b - d_{gb} g_b, \tag{9}$$

$$\frac{\partial g_v}{\partial t} = \nabla \cdot \left(D_{gv} \nabla g_v + K \cdot p \nabla g_v \right) + E_{gvb} c_b + E_{gvc} c_c, \\ - g_v (d_{gv} + d_{gvc} c_v) \tag{10}$$

$$\frac{\partial n}{\partial t} = \nabla \cdot D_n \nabla n + E_n c_v - d_n n, \tag{11}$$

where $m = m_f + m_c + m_b$ is the total tissue density.

To model the effect of ultrasound we adopt the idea presented in a previous mathematical model of VEGF diffusion in solid tumors including the effect of interstitial convection on proangiogenic and antiangiogenic factor concentrations [44]. Thus we introduce in (10) the contribution of interstitial fluid velocity **u** as follows:

$$\frac{\partial g_v}{\partial t} = \nabla \cdot D_{gv} \nabla g_v + E_{gvb} c_b + E_{gvc} c_c - g_v (d_{gv} + d_{gvc} c_v), \\ - \nabla \cdot \left(\mathbf{u} \, g_v \right) \tag{12}$$

where **u** satisfies the Darcy's law,

$$\mathbf{u} = -K\nabla p, \tag{13}$$

with K being the hydraulic conductivity of the interstitium and p is the interstitial fluid pressure. In view of (13), (12) obtains the form:

$$\frac{\partial g_v}{\partial t} = \nabla \cdot \left(D_{gv}\nabla g_v + Kg_v\nabla p \right) + E_{gvb}c_b + E_{gvc}c_c$$
$$- g_v(d_{gv} + d_{gvc}c_v). \tag{14}$$

According to a previous study on the estimation of flow properties on porous media [45], for a fluid-saturated medium subjected to a small amplitude oscillatory pressure gradient, i.e., under the ultrasound presence, the pressure fluctuation causes micro fluid flow through the sample so that to release the differential pressure. This phenomenon can be described by dynamic diffusion i.e.,

$$\frac{\partial p}{\partial t} = \nabla \cdot \left(D_p\nabla p \right), \tag{15}$$

where D_p is the diffusivity of the ultrasound acoustic pressure explained in [45].

Figure 1 depicts the area of an injured long bone where the equations (1)-(15) are applied. It should be mentioned that the present model captures the most important aspects of fracture healing. The inflammatory and remodeling phase are not included in the model.

The non-dimensionalized parameters, variables and functional forms related to migration, proliferation, chondrogenic differentiation and growth factor production given in the first 11 equations are the same as those given in [12]. When a grid volume contains a vessel, the variable c_v is set to 1, otherwise $c_v = 0$. The evolution of c_v is determined by blood vessel growth, branching and anastomosis, as proposed by [12].
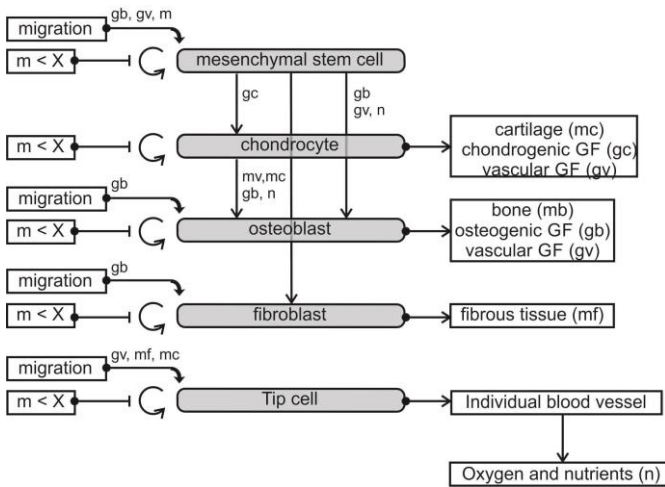

Fig. 1. Schematic overview of the hybrid model [12]. GF: growth factor, $m=mf + mc + mb$: total tissue density, X: maximum tissue density which allows for proliferation. The involvement of a variable in a regeneration subprocess is indicated by showing the name of that variable next to the arrow representing that particular subprocess.

The approach for modeling the blood vessel network is Blood vessel growth is modeled by solving the tip velocity equations that describe the movement of the corresponding tip cell [12, 13]. Branching i.e., new tip creation, occurs for high VEGF concentrations and anastomosis when a tip cell meets a blood vessel i.e., when the tip cell reaches a grid volume with $c_v = 1$.

A. Implementation details

The system of the 12 partial differential equations is numerically solved with the method of lines (MOL). Spatial discretization of the PDEs is implemented using the finite volume method to ensure mass conservation and non-negativity
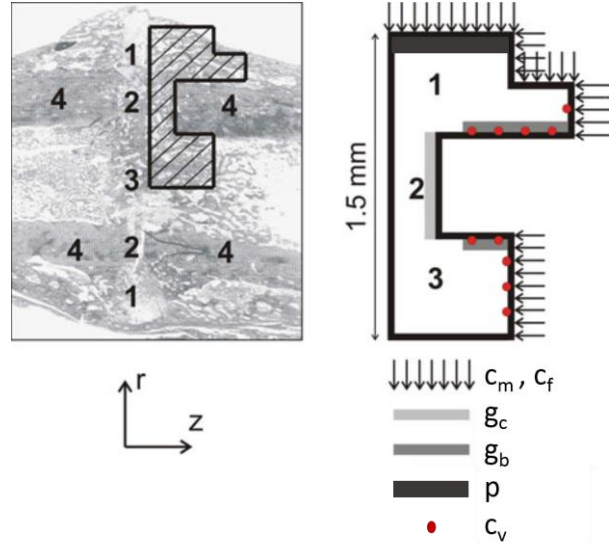

Fig. 2 Model of callus geometry derived from one fourth of real fracture callus geometry at postfracture week 3 [36] due to symmetry [12] (1) periosteal callus; (2) intercortical callus; (3) endosteal callus; (4) cortical bone. cells (Right) Boundary conditions; c_m: mesenchymal stem cells; c_f: fibroblasts; g_c: chondrogenic growth factors; g_b: osteogenic growth factors; c_v:endothelial cells p: interstitial fluid pressure.

of the variables [46]. The model is solved on a 2D grid with a grid cell size of 25 μm. The derived ordinary differential equations (ODE) are integrated in time using ROWMAP, a ROW-code of order 4 with Krylov techniques for large stiff ODEs [47]. More details can be found in [12].

B. Geometrical model of bone healing

Numerical calculations were performed on a spatial domain derived from a real callus geometry of a standardized femoral rodent fracture [48]. The geometry of the fracture callus, the initial positions of the endothelial cells and the boundary conditions are depicted in Fig. 2. The values of the initial and boundary conditions are based on [49]. No-flux boundary conditions are considered for all variables, except for those depicted in Fig. 2.

Due to symmetry issues only one-fourth of the domain is considered. Initially the callus is assumed to consist of fibrous tissue i.e., $m_f^{init} = 10\,\text{mg/ml}$. tissue i.e., $m_f^{init} = 10\,\text{mg/ml}$.
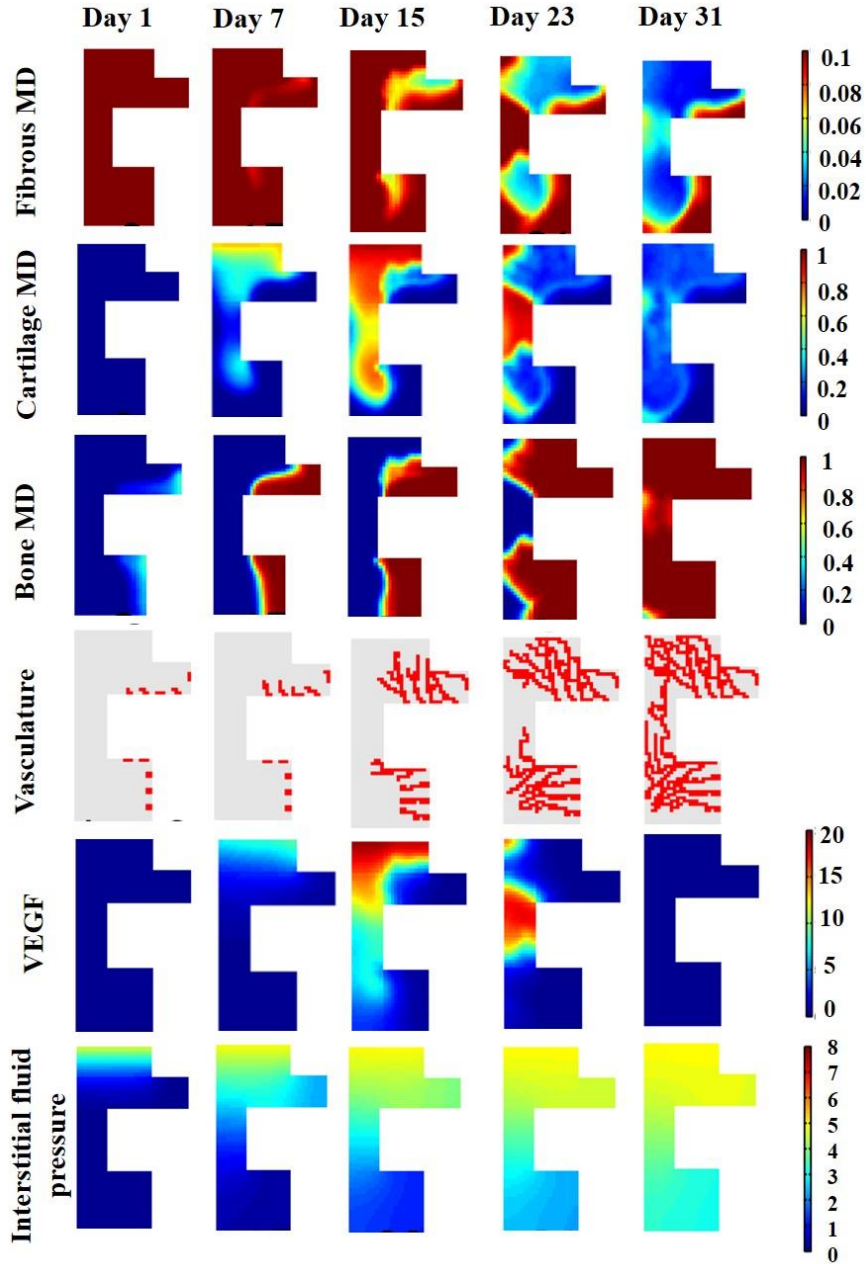
Fig. 3. Predicted spatiotemporal evolution of fibrous tissue, cartilage bone matrix density (MD, ×0.1g/ml), vasculature and VEGF under the presence of Ultrasound. D_p=0.002 and K= 0.1. The spatiotemporal evolution of the interstitial fluid pressure of ultrasound is also presented.

Mesenchymal stem cells and fibroblasts are also assumed to be released into the callus tissue from the periosteum, the surrounding tissues and the bone marrow ($c_m^{bc} = 2 \times 10^4$ cells/ml, and $c_f^{bc} = 2 \times 10^4$ cells/ml) during the first 3 postfracture (PF) days [49]. An initial amount of chondrogenic growth factors is assumed at the degrading bone ends ($g_c^{bc} = 2 \times 10^4$ mg/ml) during the first 5 PF days. Osteogenic growth are also delivered through the cortex factors during the first 10 PF days ($g_b^{bc} = 2 \times 10^4$ mg/ml). The initial positions of the tip cells are shown in Fig. 2. Endothelial cells leave the callus domain freely [49]. The periosteal region which is in close contact with the soft tissues serves as a source of acoustic pressure of ultrasound (p = 5 mmH) in order to simulate transducers' application during axial ultrasound transmission.

C. Sensitivity analysis

In [12] an extensive convergence analysis on the grid cell size and time step size has been presented as well as a sensitivity analysis on the parameters that are related to angiogenesis. Since no specific values are reported in the literature for the newly introduced variables D_p and K for bone, we investigate herein the sensitivity of the model outcome to different combinations between D_p and K. Four different cases were investigated for the non-dimensional K values i.e., $K = 0.001, 0.01, 0.1, 1$. For each of these values, D_p ranged from

0.002 to 2 i.e., D_p =0.002, 0.02, 0.2, 2. The model parameters were non-dimensionalized in accordance with [12].

Regarding the newly introduced parameters they were non-dimensionalized as follows (tildes refer to non-dimensionalized parameters):

$$\tilde{D}_p = \frac{D_p T}{L^2}, \tilde{K} = \frac{KT}{L^2} P_o,$$

where T= 1 day, L =3.5 mm, P_0= 1 mmHg.

III. RESULTS

The evolution of the tissue density in the callus during normal healing with and without the presence of ultrasound for are presented in Figs. 3, 4 and 5. Figures 3 and 4 present bone healing predictions for D_p = 0.002, K=0.1 and for D_p = 2 and K=0.1, respectively. All models can successfully describe the most important features of bone healing which start with the migration of mesenchymal cells, fibroblasts and the release of growth factors into the callus from the surrounding tissues. Near the cortex and at a distance from the fracture gap the mesenchymal stem cells differentiate into osteoblasts while in the rest of the callus they differentiate into chondrocytes. When chondrocytes become hypertrophic the angiogenic and osteogenic process starts by producing vascular growth factors. Without the ultrasound effect this occurs at the first post fracture week i.e., PFW 1 in the periosteal callus which includes the first blood vessels and at PFW 2 in the endosteal callus (Fig.5). Under the ultrasound effect for D_p = 2 and K=0.1 the angiogenesis onset is not really influenced. However for D_p = 0.002, K=0.1 angiogenesis starts in the periosteal callus at day 3 PF and in the endosteal at day 8 i.e., about a week earlier than without the ultrasound effect (Figure 5).

Thereafter the vessels deliver oxygen and nutrients which leads to endochondral ossification. The gap is then gradually filled with bone while the densities of cartilage and fibrous tissue decrease. In Fig. 3 i.e., for D_p = 0.002, K=0.1, the intercortical ossification starts at around day 23. However, in both Figs. 4 and 5 i.e., for D_p = 0.2, K=0.1 and without the ultrasound effect, this occurs 5-6 days later. Meanwhile, blood vessels grow and develop a network that occupies the whole callus region and supplies the complete fracture with oxygen and nutrients. It can be seen that for D_p = 0.002 ultrasound leads to enhanced branching and anastomosis mechanisms creating faster the vascular network within the callus region. In that case bone healing is completed at around day 26 PF. However the influence for D_p = 0.2 is limited since the evolution of the vascular network is quite similar to that without the ultrasound presence. In these two cases bone healing takes around 4-5 weeks.

Figure 6 presents the blood vessel network for different values of D_p ranging from 0.002 to 2 and for K=0.1. For D_p = 2 and D_p=0.2 the tip cells move in more or less similar directions (Figs 6(a) and 6(b)). As D_p increases, blood vessels are shown to create more branches and occupy the callus area earlier. More specifically for D_p= 0.02 angiogenesis in the periosteal callus is accelerated after day 15 PF. For D_p = 0.002 angiogenesis in the periosteal callus starts earlier than the rest cases. Furthermore
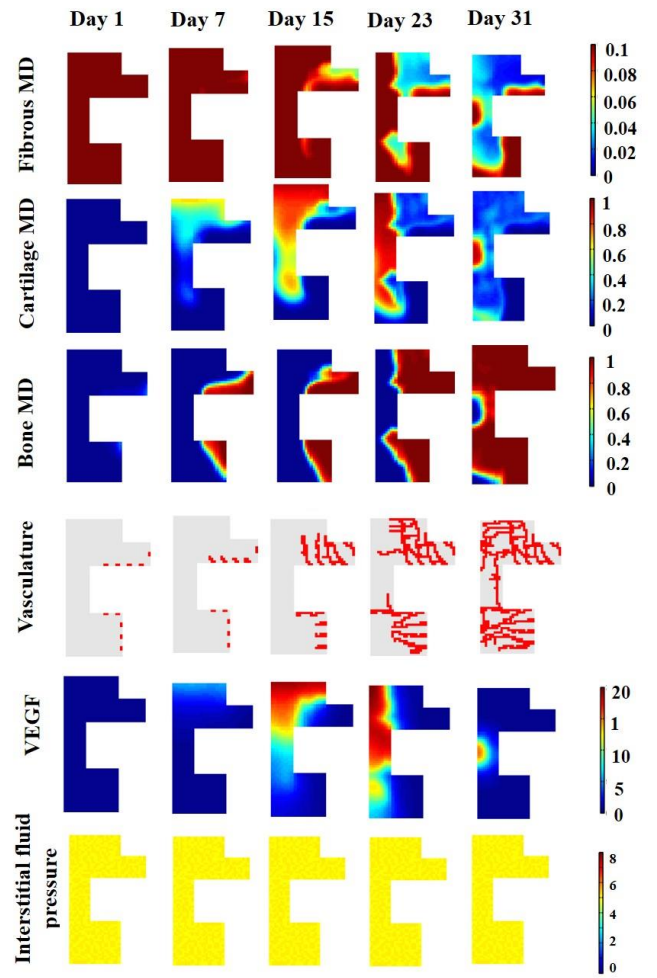

Fig. 4. Predicted spatiotemporal evolution of fibrous tissue, cartilage bone matrix density (MD, ×0.1g/ml), vasculature and VEGF under the presence of Ultrasound. D_p=2 and K= 0.1. The spatiotemporal evolution of the interstitial fluid pressure of ultrasound is also presented.

at day 23 the blood vessels have almost fully occupied in the endosteal and periosteal callus and have started invading in the intercortical callus.

Figures 7(a), (b) and (c) present the evolution of average density of osteoblasts, bone matrix density and the vascular density in the callus region for three examined combinations between D_p and K. The remaining cases have not been included in the figure since they exhibit almost similar behavior to that without the presence of ultrasound. The corresponding results derived from the model without the ultrasound effect [12] are also depicted in each figure. It can be seen that for D_p= 0.002 and K=0.1 the osteoblasts density is higher than for the other examined combinations as well as than for the model without the ultrasound effect. For higher values of D_p (even for the cases not shown in the figure) the effect of ultrasound is more pronounced in the onset of the healing process and until day 20. Thereafter the density is slightly higher than in the model
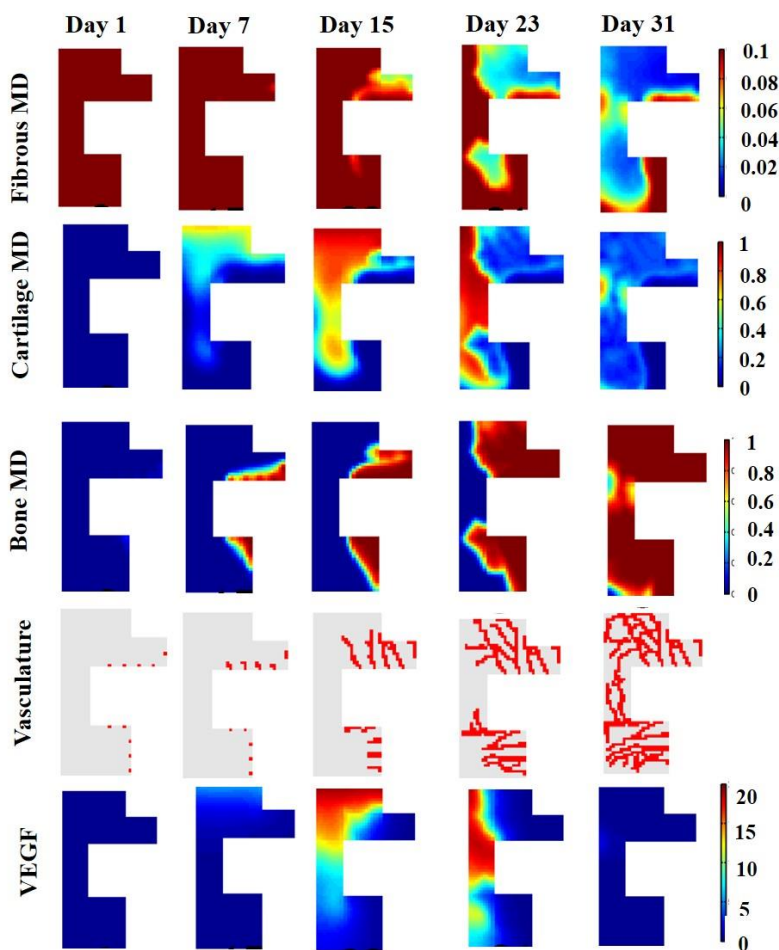
Fig. 5. Predicted spatiotemporal evolution of fibrous tissue, cartilage bone matrix density (MD, ×0.1g/ml), vasculature and vascular growth factor without the presence of Ultrasound [12].

without ultrasound for $D_p = 0.02$ and $K = 0.1$ whereas for higher D_p and lower K values it becomes almost equal or slightly lower. Similar behavior is also shown for the bone matrix and the vascular densities in the callus (Figs. 7(b), 7(c)).

More specifically at day 30 PF the bone matrix and vascular densities are equal to 93% and 36.64%, respectively, whereas under the ultrasound presence (for $D_p = 0.002$ and $K=0.1$) they are equal to 98.4% and 40.47%, respectively. These results suggest that the effect of ultrasound is more pronounced for low D_p and high K values. Table I presents the surface fraction of blood vessels in the callus throughout the healing course derived from the ultrasound models for $D_p=0.002$, $D_p=0.02$ and

TABLE I
SURFACE FRACTIONS OF BLOOD VESSELS IN CALLUS (%)

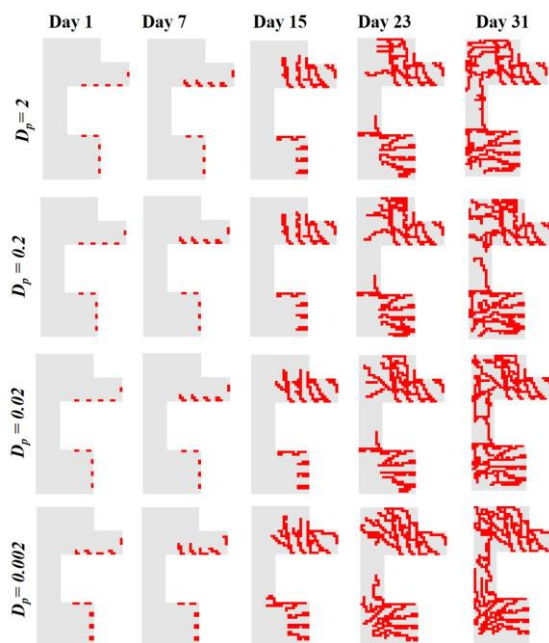|	PFW2 (DAY 14)	PFW3 (DAY 21)	PFW4 (DAY 28)
Dp=0.02 K=0.1	9.77	23.36	36.56
Dp=0.002 K=0.1	14.06	27.42	39.38
Model without US	8.05	19.53	33.91

Fig. 6 Sensitivity to the diffusivity of acoustic pressure.The evolution of vasculature is shown for $D_p=2$, $D_p=0.2$, $D_p=0.02$ and $D_p=0.002$. In this case $K=0.1$.
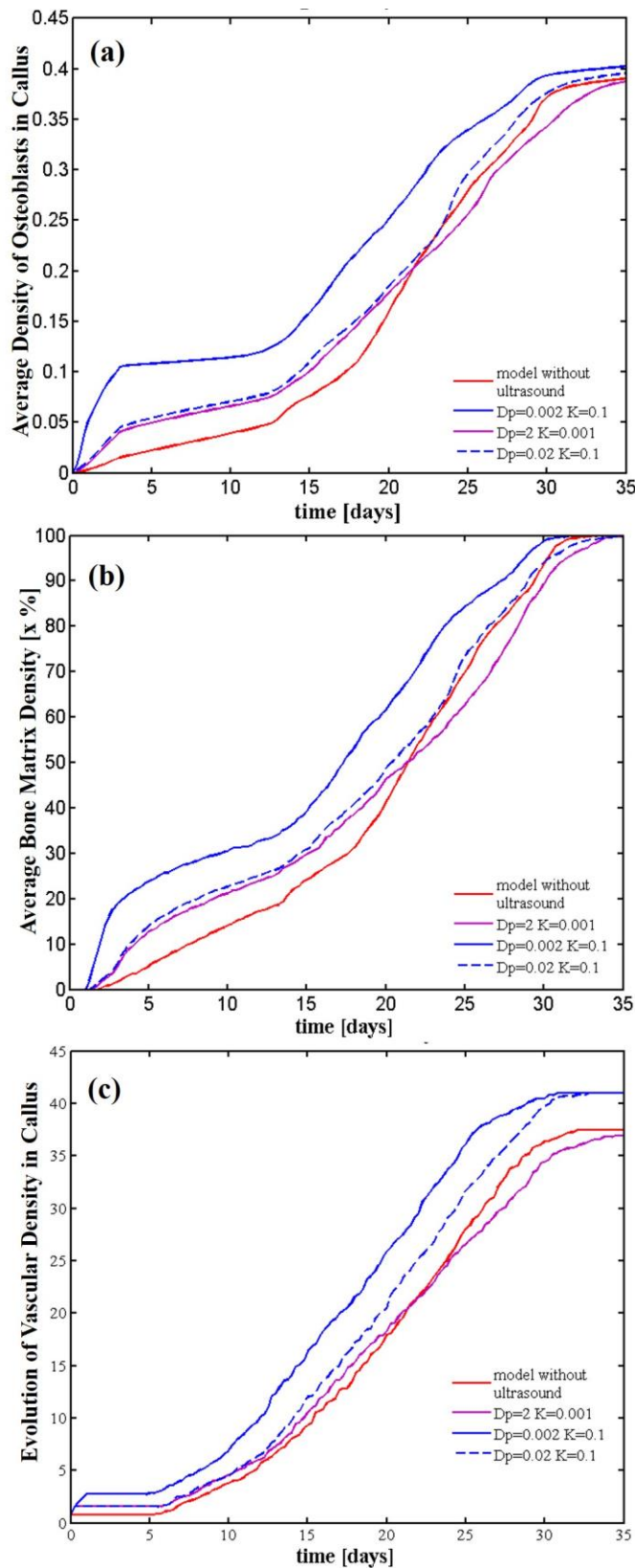
Fig. 7 Predicted temporal evolution of (a) average density of osteoblasts, (b) bone matrix density and (c) vascular density in callus for all combinations between D_p and K. The corresponding results for the model without the ultrasound effect i.e. the model of (Peiffer et al., 2011) is also presented.

K=0.1 as well as from the model without ultrasound. Augmented fractions are found for the ultrasound models compared with the model without ultrasound with the deviations to be more significant for $D_p = 0.002$ and at PFW2 and PFW3.

Figure 8 presents the temporal evolution of the tissue fractions in the periosteal, intercortical and endosteal callus derived from the newly developed model with ultrasound for $D_p = 0.002$ and K=0.1 and the model without ultrasound. Similar trends are observed in both models during the healing course. In order to calculate the tissue fractions, the spatial images are first binarised employing tissue-specific thresholds (0 when the tissue does not exist and 1 when the tissue exists in a grid cell). Then, an equal weight is assigned to the different tissues, i.e. if three tissues are contained in a grid cell, that specific grid cell area is divided by three when the tissue fractions are calculated. It can be seen that the bone fraction gradually increases as the fibrous tissue disappears and the cartilage first rises, reaches a peak and then declines. However, all processes of tissue formation and degradation in the whole callus area are affected by US presence. The fibrous tissue decreases with a higher rate in the periosteal and endosteal callus. At day 5 and 23 the fibrous tissue fraction in the endosteal callus is 72.67% and 2% respectively in the model with ultrasound as compared with 94.17% (day 5) and 10% (day 23) in the models without ultrasound. Furthermore under the influence of ultrasound cartilage formation in the endosteal callus starts at day 9 i.e., 4 days earlier than without ultrasound and is completed at day 25, i.e., 5 days later. Finally the bone tissue fraction is predicted to increase faster in the ultrasound model with the differences to be more significant in the endosteal callus. More specifically in the endosteal callus bone fraction increases from 60.83% (day 20) in the ultrasound model (vs 28.44% in the model without ultrasound) to 91.98% (day 30) (vs 86% without ultrasound). In the periosteal callus bone fraction increases from 42.58% (day 15) in the ultrasound model (vs 30.42% in the model without ultrasound) to 93.75 % (day 25) (vs 85.42% without ultrasound).

IV. DISCUSSION

In this work we presented for the first time a hybrid mathematical model for deriving bone healing predictions under the effect of ultrasound. Since the exact mechanisms by which ultrasound accelerates bone healing are unknown the aim of this model was also to provide novel insights and fundamental understanding of the influence of ultrasound on bone regeneration and angiogenesis.

The model was based on the one described in [12] and was further extended by i) including an additional equation describing the spatiotemporal evolution of the acoustic interstitial fluid pressure and ii) appropriately modifying the equation that describes the spatiotemporal evolution of VEGF. Ultrasound was assumed to primarily affect VEGF transport which is in accordance with previous in vitro studies on human cells [35, 36].
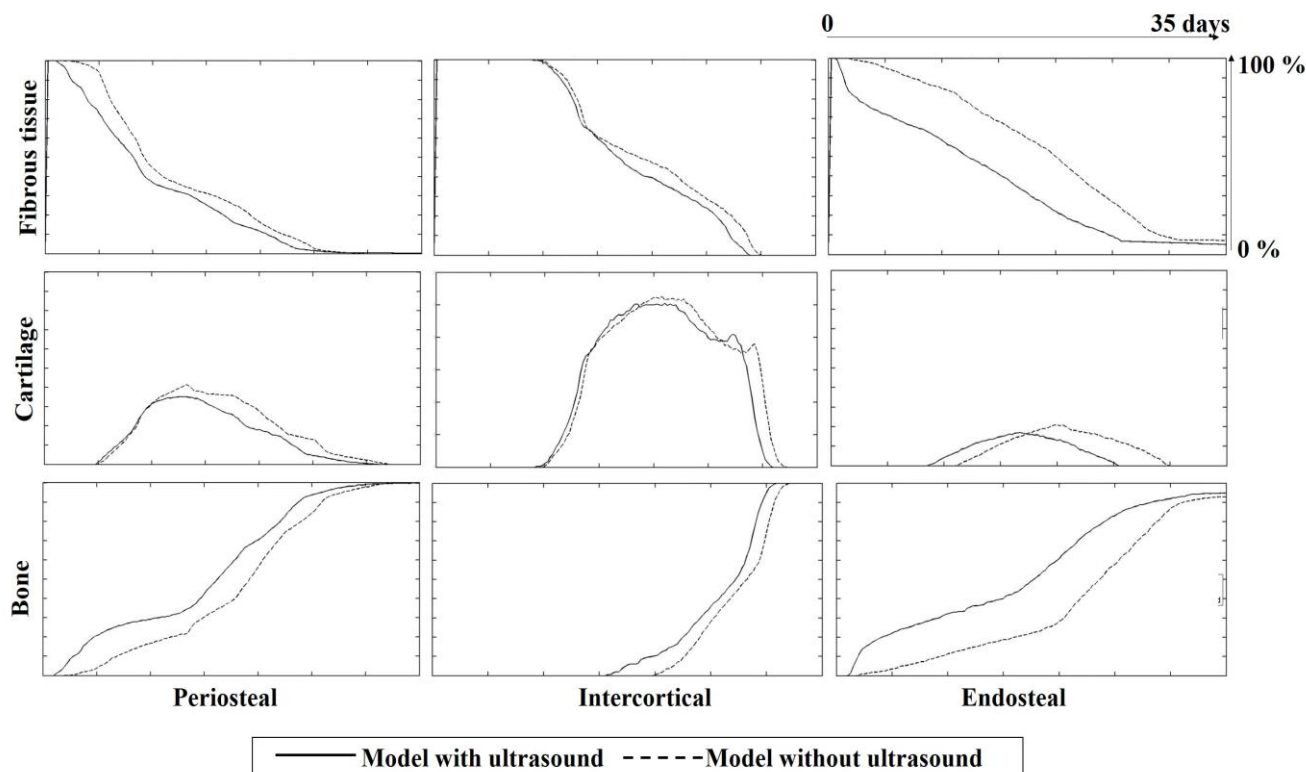
Since no values are reported in the literature for the

Fig. 8. Prediction of the temporal evolution of the bone cartilage and fibrous tissue fractions (%) in the periosteal, intercortical and endosteal callus derived from the newly developed model with ultrasound for D_p=0.002 and K=0.1 and the model without ultrasound [12].

parameters D_p, and K for ultrasound transmission in bone, an extensive sensitivity analysis of the model's outcome was performed for different combinations of diffusivities ranging from 0.002 to 2 and hydraulic conductivities ranging from 0.1 to 1. It should be noted that these values are non-dimensionalized in accordance with [12]. The values of the parameter K were at the order to those presented in the mathematical model of [44] describing the effect of the interstitial fluid pressure on angiogenic behavior in solid tumors. The values of the parameter D_p were chosen at the order of the diffusion coefficients presented in the model of [12].

In all the examined cases the model was able to capture significant events of the normal fracture healing process such as intramembranous and endochondral ossification. Ultrasound was found to have the most significant effect in bone healing mechanisms for D_p=0.02 and D_p=0.002 and for K=0.1 i.e., for the lower diffusion coefficients and the highest hydraulic conductivity. In these cases stable gradients of interstitial acoustic pressure were observed i.e., the ultrasound stimulation was heterogeneous. However, higher D_p values yield almost immediately a uniform acoustic pressure density in the callus (equal to the applied boundary condition p=5) meaning that everything is stimulated/or inhibited in the same way. Therefore our findings suggest that ultrasound significantly influences the bone healing mechanisms when the interstitial acoustic pressure a) is heterogeneous and b) highly affects VEGF diffusion i.e., for high values of K.

On the other hand when the diffusion coefficient of the interstitial pressure is increased and VEGF transport is less affected (i.e., for higher D_p and lower K) ultrasound was found to enhance osteoblast average density and bone formation in callus for the first 2 PFW i.e., during the reparative phase of healing. Nevertheless during the last healing stages ultrasound had either no or even a slightly negative effect.

Moreover higher amounts of blood vessels were observed at weeks 2-4 in the ultrasound models (D_p=0.02 and D_p=0.002 aand K=0.1) at weeks 2-4. This enhancement effect was more pronounced for lower D_p. Previous experimental works report that ultrasound enhances the liberation of the vascular endothelial growth factor (VEGF) and this could be the reason of the augmented levels of vascularity on the site and the enhanced angiogenesis. Increased new blood vessel formation due to ultrasound have been also reported in various animal fractures using techniques such as Doppler assessment [39, 26].

Calculations of the volume fractions of all tissues in the endosteal, periosteal and intercortical callus during the healing course showed a more rapid decrease in the fibrous tissue volume fraction and an increased bone formation rate and thus increased levels of bone matrix. These findings are in agreement with previous animal studies on a sheep osteotomy which report that transosseous ultrasound application leads to an increase in bone matrix density and accelerated healing time [43]. Increased levels of bone density due to ultrasound are also reported in [27, 51].

The qualitative evolution of cartilage is similar for both models with and without ultrasound (Figure 8). However in the ultrasound model: i) the cartilage fraction in the periosteal callus decreases faster and ii) in the endosteal callus cartilage

formation and degradation occurs earlier than in the model without the ultrasound effect. These observations may be indicative of an earlier endochondral ossification and are consistent with several in vitro and in vivo studies reporting that US leads to earlier chondrogenesis and cartilage hypertrophy causing earlier endochondral ossification [39]. In this respect a possible US affected pathway that could be suggested from the proposed model (i.e., by accounting a direct US influence on the VEGF transport) may that of the endochondral ossification [39].

The osteoblast density was also found to be about 10% greater in the ultrasound model from PFW1 to PFW4, which is also reported in previous experimental studies [50-54]. Nevertheless no safe conclusions can be drawn for this enhancement influence since this is downstream effect and has not been explicitly modeled herein.

Leung et al., [55] applied LIPUS on human periosteal cell culture and found that it has a negative effect on osteoblast proliferation but enhances their differentiation through osteocytes in vitro. The authors suggested that this may be attributed to the increased levels of PGE2 release from osteocytes. This could possibly explain our finding that for high D_p and low K ultrasound has no or slightly negative effect in bone healing mechanisms.

The remodeling phase of bone healing is not addressed by the proposed model. Nevertheless the direct effects of US on the cellular processes involved in the bone remodeling stage of healing have not been elucidated yet. Mundi et al. [1] suggest the hemodynamic shear stress caused by the LIPUS-induced increase in blood pressure as well as the subsequent increased fluid flow and fluid turbulence at the fracture site to play significant role in bone remodeling by causing the gathering of osteoprogenitor cells from the marrow.

The effects of the mechanical environment in the callus were also not examined in this work. However, variations in the stability of the fracture and the motion between the bone fragments may influence cell migration, cell proliferation or matrix formation and the angiogenic response [56]. In addition previous studies have found increased mechanical stimulus during distraction osteogenesis [57]. Cell differentiation and tissue development may be also sensitive to alterations in the mechanical environment.

As previously mentioned ultrasound has been experimentally found to affect multiple cellular mechanisms during bone healing. In this respect we have extended by performing some initial simulations which also account for the effect of ultrasound on osteoblasts proliferation and VEGF production. Nevertheless further investigation is needed in order to draw safe conclusions and determine whether certain scenarios of US affected mechanisms are more plausible than others. Furthermore several ultrasonic parameters that have been reported to influence the effect of US on fracture healing such as temperature changes, frequency, intensity, dose, duration and timing of US application are not considered herein. However, models that also account for the mechanical environment and the interaction of the acoustic pressure with such physical parameters would provide significant information and constitute a valuable extension of the proposed framework.

CONCLUSIONS

In this work we incorporate for the first time the effect of ultrasound on a previously developed hybrid model of bone regeneration. The results made clear that when the interstitial acoustic pressure is heterogeneous and the effect on VEGF transport is high, ultrasound plays a significant role in the underlying healing mechanisms and lead to accelerated bone regeneration. However, when the pressure rapidly reaches a plateau and VEGF transport is less affected, the effect is more pronounced only during the reparative phases of bone healing. In conclusion mathematical models accounting for the multifaceted effect of ultrasound could be a useful tool for the orthopedic surgeons assisting them to predict the treatment outcome, early diagnose complications and continuously monitor the progress of healing course.

REFERENCES

[1] R. Mundi, S. Petis, R. Kaloty, V. Shetty, M. Bhandari (2009). "Low-intensity pulsed Ultrasound: Fracture healing." *Ind. Journ. Orthopaed.* 43(2), pp. 132-140.

[2] L. Claes, B. Willie (2008). "The enhancement of bone regeneration by ultrasound." *Progr. Biophy. Mole. Biol.* 93, pp. 384–98.

[3] G.J. Tortora, S.R Grabowski (2003). "Principles of anatomy and physiology." (10th ed.) Hoboken (NJ): John Wiley and Sons, Inc

[4] H.M. Frost (1989). The biology of fracture healing, part I. Clin. Orthop. Rel. Res., pp. 248-283.

[5] R. Holmes, S. Lemperle, C. Calhoun (2001). "Protected Bone Regeneration". Scientific data series in resorbable fixation, pp. 1-10.

[6] AI. Caplan (1994). "The mesengenic process: bone repair and regeneration." *Clinics in Plastic Surgery* 21, pp. 429-435.

[7] R.A. Brand and C.T. Rubin (1990). "Fracture healing." *Surg. Musc. Syst.*, 1:93, pp. 114.

[8] A.B. Plaza, C.H. Van der Meulen (2001). "A mathematical framework to study the effects of growth factor influences on fracture healing." *J. Theor. Biol.* 212, pp. 191-209.

[9] R.A.D. Carano, E.H. Filvaroff (2003). "Angiogenesis and bone repair." *Drugs Disc. Today* 8(21), pp. 980-989.

[10] L. Geris, J. Vander Sloten, H. Van Oosterwyck (2007). "Angiogenesis in Bone Fracture Healing: a Bioregulatory Model." *J Theor Biol.* 251(1), pp. 137-58.

[11] J. Street, M. Bao, L. deGuzman, S. Bunting, F.V Peale, N. Ferrara, H. Steinmetz, J. Hoeffel, J.L. Cleland, A. Daugherty, N. van Bruggen, H.P. Redmond, R.A.D. Carano, E.H. Filvaroff (2002). "Vascular endothelial growth factor stimulates bone repair by promoting angiogenesis and bone turnover." *P. Natl Acad. Sci.* USA 99(15), pp. 9656-9661.

[12] V. Peiffer, A Gerisch, D Vandepitte, O.H Van, L Geris (2011). "A hybrid bioregulatory model of angiogenesis during bone fracture healing." *Biomech. Model. Mechanobiol* (10), pp. 383–395.

[13] S. Sun, M. Wheeler, M. Obeyesekere, C.J. Patrick (2005). "A deterministic model of growth factor-induced angiogenesis." *Bull Math Biol* (67), pp. 313–337.

[14] D. Anderson, P. Thaddeus, A. Marin, J. Elkins, W. Lack, D. Lacroix (2014) "Computational techniques for the assessment of fracture repair." *Injury, Int. J. Care Injured* (45S), pp. S23-S31.

[15] L.Geris, A. Gerisch, R. Schugart (2010) "Mathematical Modeling in Wound Healing, Bone Regeneration and Tissue Engineering" *Acta Biotheor* (58), pp.355–367.

[16] S. J. Shefelbine, P. Augat, L. Claes, U. Simon (2005). "Trabecular bone fracture healing simulation with finite element analysis and fuzzy logic", *J. of Biomechanics* (38), pp. 2440-2450.

[17] L. Claes, C. Heigele (1999). "Magnitudes of local stress and strain along bony surfaces predict the course and type of fracture healing". *J. Biomech.* 32 (3), pp. 255–266.

[18] G. Chen, F. Niemeyer, T. Wehner, U. Simon, M. Schuetz, M. Pearcy, L. Claes (2009). "Simulation of the nutrient supply in fracture healing." *J. Biomech.* 42 (15), pp. 2575–2583.

[19] L. Geris, A. Gerisch, J. Vander Sloten, R. Weiner, H. Van Oosterwyck (2008). "Angiogenesis in bone fracture healing: a bioregulatory model." *J Theor Biol* (25), pp. 137–158.

[20] S. Checa, P.J. Prendergast (2009). "A mechanobiological model for tissue differentiation that includes angiogenesis: a lattice-based modeling approach." *Ann Biomed Eng.* 37(1), pp. 129-45.

[21] A. Anderson, M. Chaplain (1998). "Continuous and discrete mathematical models of tumor-induced angiogenesis." *Bull Math Biol* (60), pp. 857–900.

[22] S. Checa, P.J. Prendergast, G.N. Duda (2011). "Inter-species investigation of the mechano- regulation of bone healing: Comparison of secondary bone healing in sheep and rat." *J. Biomech.* 44 (7), pp. 1237-1245.

[23] F. Milde, M. Bergdorf, P. Koumoutsakos (2008). "A hybrid model for three-dimensional simulations of sprouting angiogenesis." *Biophys*. J 95, pp. 3146–3160.

[24] A. Qutub, A. Popel (2009). "Elongation, proliferation & migration differentiate endothelial cell phenotypes and determine capillary sprouting." *BMC Syst Biol* 3(13) pp. 1-24.

[25] F. Padilla, R. Puts, L. Vico, K. Raum (2014). "Stimulation of bone repair with ultrasound: A review of the possible mechanic effects" *Ultrasonics* (54), pp.1125–1145.

[26] W.H. Cheung, S.K Chow, M.H. Sun, Qin Ling. Kwok-Sui Leung (2011). "Low-Intensity Pulsed Ultrasound Accelerated Callus Formation, Angiogenesis and Callus Remodeling in Osteoporotic Fracture Healing." *Ultr. Med. Biol.* 37(2), pp. 231–238.

[27] C. Fung, W. Cheung, N. Pounder, A. Harrison, K. Leung K. (2012) "Effects of different therapeutic ultrasound intensities on fracture healing in rats *Ultrasound Med Biol.* 38(5), pp. 745-52.

[28] L.R. Duarte (1983). "The stimulation of bone growth by ultrasound." *Arch. Orthop. Trauma Surg*. (101), pp. 153–159.

[29] K.H Yang, J. Parvizi, S.J. Wang. "Exposure to low-intensity ultrasound increases aggrecan gene expression in a rat femur fracture model." (1996) *J Orthop Res.*14(5), pp. 802–9.

[30] S. Jingushi, M.E. Joyce, M.E. Bolander (1992) "Genetic expression of extracellular matrix proteins correlates with histologic changes during fracture repair." *J Bone Miner Res* (7), pp. 1045–1055.

[31] Parvizi, V. Parpura, R.R. Kinnick, J.F. Greenleaf (1997). "Low intensity ultrasound increases intracellular concentration of calcium in chondrocytes." *Trans Orthop Res Soc* (22), pp. 465.

[32] A. Wiltink, P.J. Nijweide, W.A Oosterbaan, R.T. Hekkenberg, P.J.M. Helders (1995). "Effect of therapeutic ultrasound on endochondral ossification." *Ultrasound Med Biol* (21). pp. 121–127.

[33] C-C. Wu, D.G. Lewallen, M.E. Bolander, J. Bronk, R. Kinnick, J.F Greenleaf (1996). "Exposure to low intensity ultrasound stimulates aggrecan gene expression by cultured chondrocytes." *Trans Orthop Res Soc* (21), pp. 622.

[34] Z.J. Zhang, J. Huckle, C.A Francomano, R.G Spencer (2003). "The effects of pulsed low-intensity ultrasound on chondrocyte viability, proliferation, gene expression and matrix production". *Ultrasound Med Biol* (29), pp. 1645–1651.

[35] P. Reher, N. Doan, B. Bradnock, S. Meghji, M. Harris (1999). "Effect of ultrasound on the production of IL-8, basic FGF and VEGF." *Cytokine* (11), pp. 416–423.

[36] N. Doan, P. Reher, S. Meghji, M. Harris (1999). "In vitro effects of therapeutic ultrasound on cell proliferation, protein synthesis and cytokine production by human fibroblasts, osteoblasts, and monocytes." *J Oral Maxillofac Surg*. (57), pp. 409–419, 1999.

[37] N.M. Rawool, B.B. Goldberg, F. Forsberg, A.A Winder, E. Hume (2003). "Power Doppler assessment of vascular changes during fracture treatment with low-intensity ultrasound." *J Ultrasound Med* (22), pp. 145–153.

[38] O. Erdogan, E. Esen (2009). "Biological aspects and clinical importance of ultrasound therapy in bone healing." *J. Ultrasound Med.* 28 (6), pp. 765-76.

[39] P. Martinez de Albornoz, A. Khanna, U. G. Longo, F. Forriol, N. Maffulli (2011). "The evidence of low-intensity pulsed ultrasound for in vitro, animal and human fracture healing" *British Medical Bulletin* 100(1), pp. 39.

[40] P.J. Polverini, R.S. Cotran, M.A. Gimbrone, E.R. Unanue (1977). "Activated macrophages induce vascular proliferation." *Nature* (269), pp. 804-806.

[41] S.J. Leibovich (1984). "Mesenchymal cell proliferation in wound repair." In: Hunt, T. K.; Heppenstall, R. B.; Pines, E.; Rovee, D., eds. Soft and hard tissue repair. New York: Praeger, pp. 329-345.

[42] R. Ramli, P. Reher, M. Harris, S. Meghji. (2009) "The effect of ultrasound on angiogenesis: an in vivo study using the chick chorioallantoic membrane." *Int J Oral Maxillofac Implants*. 24(4):591-6.

[43] V. Protopappas, M. Vavva, D. Fotiadis, K. Malizos. (2008) "Ultrasonic Monitoring of Bone Fracture Healing" IEEE Trans. Ultras., Ferroel., and freq. cont., (55), pp. 1243-1255.

[44] C. Phipps and M. Kohandel (2011). "Mathematical Model of the Effect of Interstitial Fluid Pressure on Angiogenic Behavior in Solid Tumors", *Comp. and Math. Meth in Med,* pp. 1- 9.

[45] C. Xu, J.M. Harris, Y. Quan (2006). "Estimating flow properties of porous media with a model for dynamic diffusion." Geoph. Dep. New Orleans, Annual Meeting, pp. 1831-1835.

[46] A. Gerisch, M.A.J. Chaplain (2006). "Robust numerical methods for taxis-diffusion-reaction systems: applications to biomedical problems." Math. Comput. Modell. (43), pp. 49–75.

[47] R. Weiner, B.A. Schmitt, H. Podhaisky (1997). "ROWMAP- a ROW-code with Krylov techniques for large stiff ODEs." *Appl. Num. Math.* (25), pp. 303–319.

[48] L.J. Harrison, J.L Cunningham, L. Stromberg, A.E Goodship (2003). "Controlled induction of a pseudarthrosis: a study using a rodent model." *J. Orthop. Trauma* (17), pp. 11–21.

[49] L. Gerstenfeld, D. Cullinane, G. Barnes, D. Graves, T. Einhorn (2003). "Fracture healing as a post-natal developmental process: molecular, spatial, and temporal aspects of its regulation."*J. Cell. Biochem.* 88(5), pp. 873-84.

[50] J. Ryaby, J. Mathew, A. Pilla (1991). "Low-intensity pulsed ultrasound modulates adenylate cyclase activity and transforming growth factor beta synthesis." In: Brighton CT, Pollack SR (eds) Electromagnetics in biology and medicine. San Francisco Press, San Francisco, pp 95– 100.

[51] S. Warden, J. Favaloro, K. Bennell, J. McMeeken, K. Ng, J. Zajac, J. Wark (2001). "Low-intensity pulsed ultrasound stimulates a bone-forming response in UMR-106 cells" *Biochem. Biophys. Res. Commun.* 286 (3), pp. 443–450.

[52] J. Ryaby, J. Mathew, P. Duarte-Alves (1992). "Low intensity pulsed ultrasound affects adenylate cyclase and TGF-b synthesis in osteoblastic cells." *Trans Orthop Res Soc* (17), pp. 590.

[53] K. Ebisawa, K. Hata, K. Okada, K. Kimata, M. Ueda, S. Torii, H. Watanabe (2004). "Ultrasound enhances transforming growth factor betamediated chondrocyte differentiation of human mesenchymal stem cells" *Tissue Eng.* 10 (5–6), pp. 921–929.

[54] J.N. Ridgway, S. Kaneez, J.M. Unsworth, A.J. Harrison (2005) "Osteogenic gene expression in response to pulsed low intensity ultrasound". Presented at 51st Annual Meeting of the Orthopaedic Research Society [poster] available: http://www.ors.org/Transactions/51/0857.pdf

[55] K. Leung, W. Cheung, C. Zhang, K. Lee, H. Lo (2004). |Low intensity pulsed ultrasound stimulates osteogenic activity of human periosteal cells.| Clin Orthop Relat Res (9), pp. 418:253.

[56] S. Perren, J. Cordey (1980). "The concept of interfragmentary strain." In: Uhthoff, H.K., (Ed.), Current Concepts of Internal Fixation of Fractures, Springer, Berlin, pp. 63—77

[57] M. Sato, T. Ochi, T. Nakase, S. Hirota, Y. Kitamura, S. Nomura and N. Yasui (1999) "Mechanical Tension-Stress Induces Expression of Bone Morphogenetic Protein (BMP)-2 and BMP-4, but Not BMP-6, BMP-7, and GDF-5 mRNA, During Distraction Osteogenesis" *J. Bone Miner Res.* pp. 1084-95.